Proceedings of the 25th International Conference on
Port and Ocean Engineering under Arctic Conditions
June 9-13, 2019, Delft, The Netherlands

The effect of ship bow shape on ridge resistance in a narrow ridge

Hanyang Gong, Arttu Polojärvi, Jukka Tuhkuri
Aalto University, School of Engineering, Department of Mechanical Engineering, P.O. Box 14300, FI-00076 Aalto, Finland

ABSTRACT

This paper studies the effect of ship bow shape on ridge resistance in a narrow ridge by using 3D discrete element method (DEM). A series of simulations on a ship passage through a narrow ridge are performed with different bow shapes, characterized by the bow angles: waterline angle, stem angle, and flare angle. By analysing the relation among the bow angles, the simulated ridge resistance, and the work needed for passing a ridge, we observe that the peak ridge resistance and the work both are increasing with an increase in any of the bow angles. The general features of the ridge deformation patterns are observed to be related to the ridge resistance records.

KEY WORDS: Bow shape; Bow angles; Ice ridge resistance; Ridge deformation; DEM.

INTRODUCTION

Ships in ice covered seas commonly encounter ice ridges. Due to this, the ridge resistance must be considered in route planning and in the early stage of ship bow design. Comparing to the studies on the level ice resistance (Lindqvist, 1989; Riska, 1997; Yamaguchi et al., 1997; Myland and Ehlers, 2016; Li et al., 2018), research on how the ship bow shape affects the ice ridge resistance are rare. Only a limited number of research work (Keinonen, 1979; Malmberg, 1983) give analytical solutions of ridge resistance using the main dimensions of a ship, the ridge thickness, and material properties of the ice ridge with an infinite width (along ship's heading direction). However, such approaches do not give the resistance in a ridge with the finite width: The ridge resistance is affected by the ridge width as long as the width is smaller than the waterline length of a ship passing through the ridge (Gong et al., 2017 and 2018). In addition, there is still a lack of detailed knowledge on how the bow shape affects the ship interaction with a narrow ridge. This paper uses a 3D discrete element method (DEM) to simulate a ship passage through a narrow ridge. Simulations are performed with a number of different ship bow shapes.

NUMERICAL SIMULATIONS

The study reported here is performed using the in-house 3D DEM code developed by Aalto University Ice Mechanics Group. Detailed description of the code and its validation are presented by Polojärvi and Tuhkuri (2009) and Polojärvi et al. (2012). We have applied the

code to simulate a ship passage through an ice ridge (Gong et al., 2017) and to study the effect of ridge width on ice ridge resistance (Gong et al., 2018). A reader can find the entire description of the simulation setup from Gong et al. (2017). Here we only summarize some details of the setup relevant to this study.

Figure 1a presents the simulation basin with the coordinate system. The centre line of the ship is parallel to the x-axis and aligns with the centre line of the basin and the plane of symmetry at $y = 0$. An ice ridge highlighted in light blue is constrained by the plane of symmetry, an ice cover mimicked by a rigid plate at $z = 0$, and the basin wall at $y = -l/2$, where l is the ridge length. A half model, the part where $y < 0$, is modelled. This half model has been proved to be equivalent to half of the whole model (Gong et al., 2017), and thus all results in this paper are obtained from models that utilize the plane of symmetry at $y = 0$ and the domain $l/2 = 30$ m.

The scope of this study is limited to a narrow ridge. The ice ridge has the keel component only, and ridge sail or consolidated layer are not modelled. Figure 1b shows a triangular ridge cross section with depth h and width w of 5 m and 17.3 m, respectively, and keel angle of 30°. The ridge is non-cohesive and consists of rigid and cuboid-shaped blocks having thickness of 0.3 m. The other two dimensions of the blocks vary randomly but following the shape distribution given by Kulyakhtin and Høyland (2014), with a restriction that the aspect ratio of the blocks varies from 0.6 to 15. The same ridge configuration is used in all simulations. Parameters related to the ice ridge are listed in Table 1.

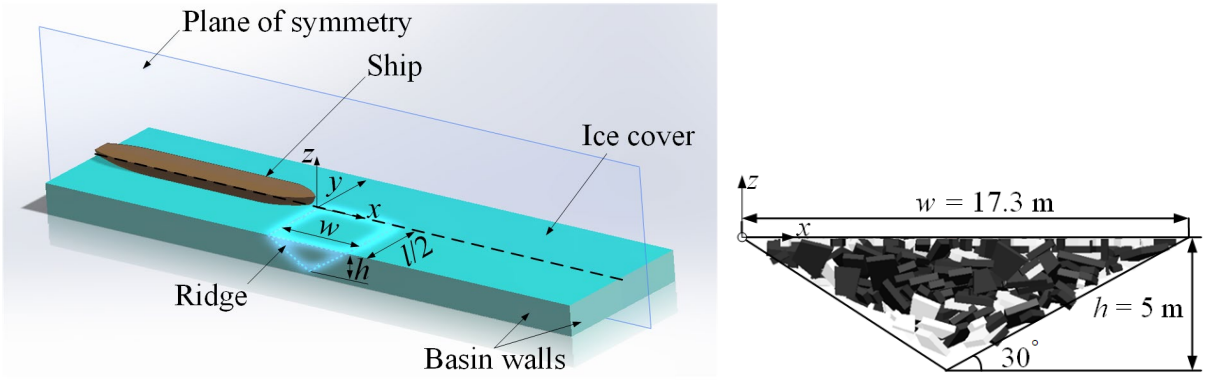

(a) (b)

Figure 1. (a) The simulation domain and the coordinate system. w is ridge width, l is ridge length, and h is ridge depth. (b) The dimensions of the narrow ice ridge with a triangular cross section.

Ship bow shapes

Wedge shaped bows are common for ice-going ships (Yamaguchi, 1997). In order to study how the ship bow shape affects ridge resistance, ship hulls with wedge shaped bows and sterns – formed with flat plates – are used (Figure 2). The main dimensions of the ship hulls are those of MT Uikku, which also has a wedge shaped bow, and is used here as a reference ship. Table 1 gives the main dimensions of MT Uikku.

The bow shape can be characterized by the bow angles: waterline angle α, stem angle φ, and flare angle ψ, shown in Figure 2 (Kujala and Riska, 2010). These three angles are related through

$$\psi = \arctan(\tan\varphi / \sin\alpha) \quad (1)$$

In this paper, following the Finnish-Swedish Ice Class Rules (TRAFI, 2010), α and φ of MT Uikku are measured as 25.2° and 29.7°, respectively, from the waterline at a distance of $B/4$, a quarter of breadth B, from the centre line of a ship.

Six different simple hull forms were generated. The bow angles of these hulls are given in Table 2 and two examples are shown in Figure 2. The bow angles of MT Uikku are listed as reference. The hull forms 1 – 4 have equal waterline angles, $\alpha = 25.2^{\circ}$, as in MT Uikku, but different stem and flare angles, φ and ψ, respectively; the hull forms 4 – 6 have vertical bows, $\varphi = \psi = 90^{\circ}$, but varying α.

With bow angles changing, the bow length L_{bow} may also change (Figure 2 and Table 2) potentially affecting the ridge resistance and the process of ship indenting a ridge. The bow lengths are illustrated in Figure 2, showing the waterline length of the bow region L_b divided into L_{bow} and the bow intermediate length (IACS, 2016). The simple hull form in Figure 2c does not have a bow intermediate.

Table 1. The main parameters used in simulations.

	Parameter	Unit	Value
Contact	Penalty term	-	$1 \cdot 10^{7}$
	Damping constant	-	$5 \cdot 10^{5}$
	Time step	s	$5 \cdot 10^{-5}$
Ice blocks	Thickness	m	0.3
	Block aspect ratio	-	0.6…15
	Ice-ice friction coefficient μ_i	-	0.3
	Mass density	kgm^{-3}	920
Water	Mass density	kgm^{-3}	1010
Ridge (keel)*	Ridge depth h	m	5
	Ridge angle θ	°	30
	Ridge width w	m	17.3
	Ridge length $l/2$	m	30
MT Uikku	Waterline length L	m	150
	Waterline length of the bow region L_b	m	40
	Parallel midbody length L_m	m	67.5
	Breadth B	m	22
	Draft T	m	9.5
	Ship-ice friction coefficient μ_s	-	0.1
	Ship velocity v_{ship}	ms^{-1}	1

*all values refer to the initial ridge geometry. l refers to full ridge model.

Table 2. The list of bow angles and bow length of MT Uikku and simple hull forms used.

Parameter	MT Uikku	Simple hull forms					
		1	2	3	4	5	6
α [°]	25.2	25.2	25.2	25.2	25.2	15	45
φ [°]	29.7	22.7	29.7	52.7	90	90	90
ψ [°]	53.3	45	53.3	72	90	90	90
L_{bow} [m]	20	24	24	24	24	41	11

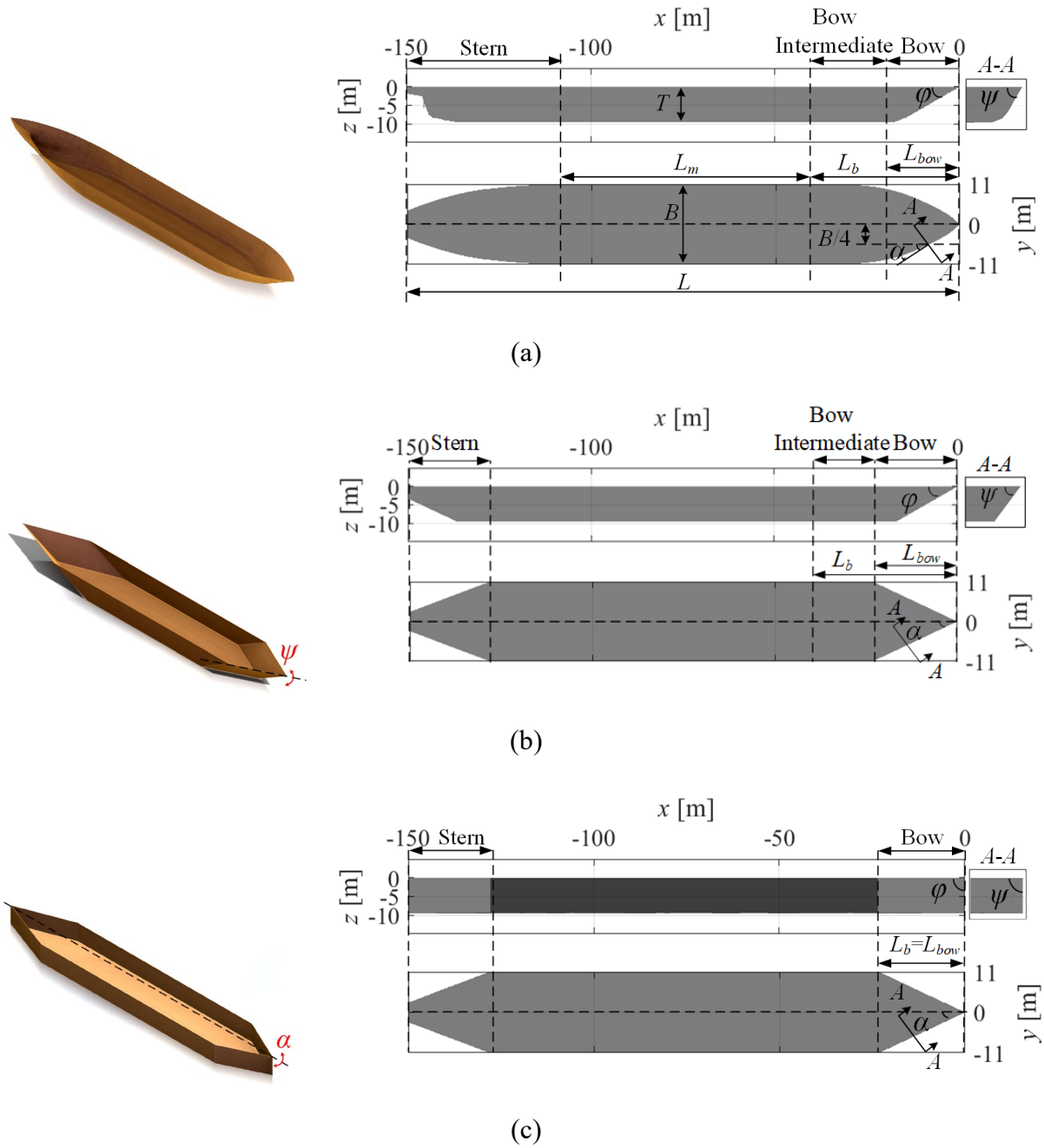

Figure 2. Ship hull forms used in the simulations. Ship breadth B, draft T, waterline length L, waterline length of bow region L_b, and bow length L_{bow} are shown. (a) MT Uikku. (b) A simple hull form resembling MT Uikku. (c) A simple hull form with a vertical bow.

RESULTS AND DISCUSSION

This section presents the results of our study by showing the ridge resistance records for models with different bow shapes and by discussing the effect of bow angles on ridge resistance and the work needed for passing a ridge. In addition, we use snapshots from the simulations to analyse the relations among the bow shape, the ridge resistance, the work, and the ridge deformation patterns.

The effect of flare angle ψ and stem angle φ on ridge resistance

Figure 3a shows the ridge resistance R as a function with ship displacement δ for MT Uikku and for simple hull forms 1 – 4 defined in Table 2 (equal α but different ψ and φ). For each

case, the peak resistance R^p is defined as the maximum of the running average calculated with window size of δ = 6 m on the corresponding unfiltered simulation data; as a reference, the unfiltered simulation data for MT Uikku is shown in grey in Figure 2. The resistance records indicate that all the simple hulls yield a similar ridge penetration process as MT Uikku: R increases with δ until R^p, then R decreases to a constant value before vanishing once the ship passes through the ridge.

Figure 3b shows the normalised peak ridge resistance $\widehat{R}^p$ of different bow shapes and the normalised work $\widehat{W}$ done by different hulls passing through a ridge ($\delta = 0 \ldots 80$ m), normalised by R^p and W of MT Uikku, respectively, and plotted against the bow angle ψ. Both $\widehat{R}^p$ and $\widehat{W}$ are increasing approximately linearly with the increase of ψ. Similar linear relationships are found for $\widehat{R}^p(\varphi)$ and $\widehat{W}(\varphi)$. As ψ and φ increase, the ship is pushing more ice blocks horizontally than downwards; the bow is compressing the ridge rather than disintegrating it, resulting in increasing resistance and work. This figure also shows that MT Uikku has lower R^p than the simple Hull 2 ($\psi = 53.3^\circ$) resembling MT Uikku, but the work done by both hulls are similar. The work needed for a ship passing through a ridge appears less sensitive to changes in the hull form than the peak resistance.

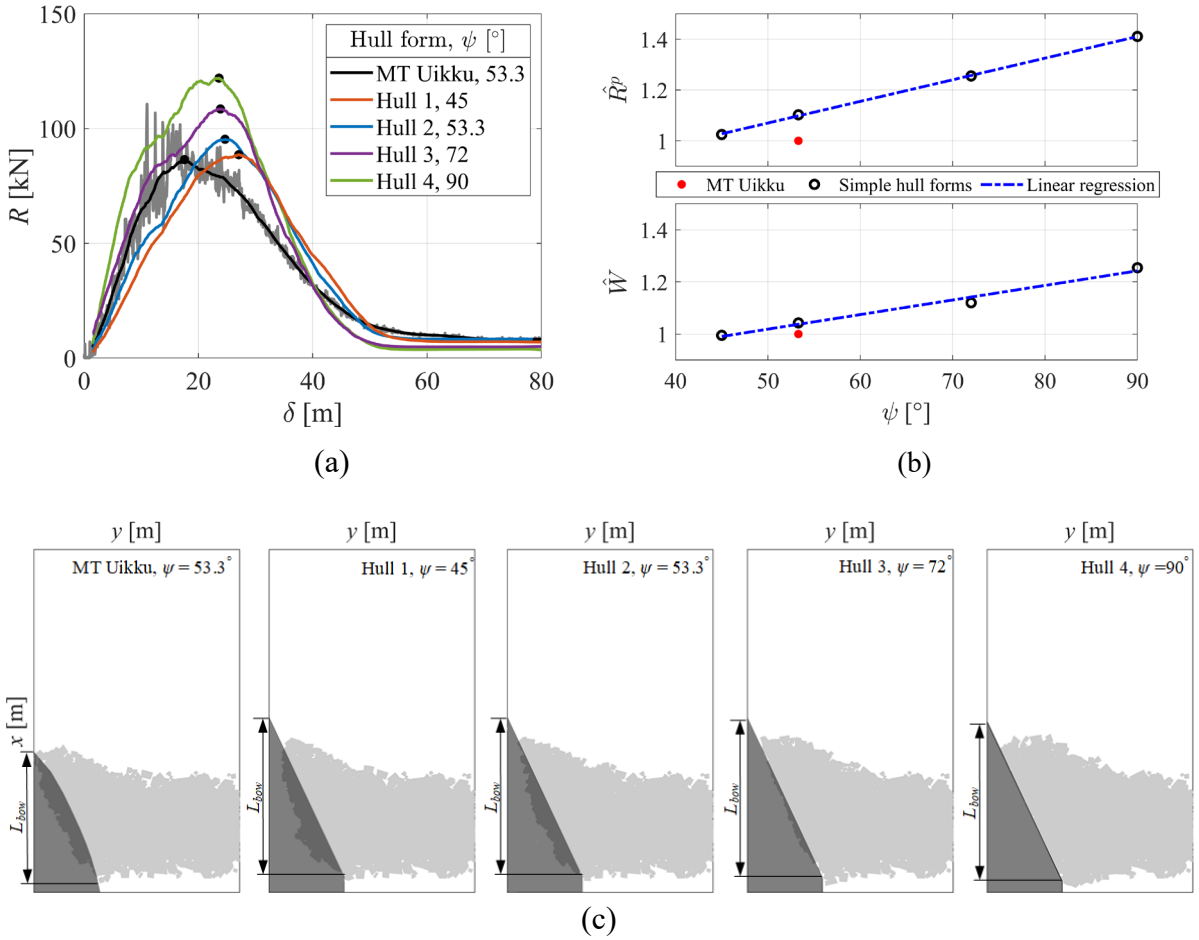

Figure 3. (a) Ridge resistance – ship displacement (R-δ) records for MT Uikku and the simple hull forms 1 – 4 (Table 2). The unfiltered data for MT Uikku is coloured in grey. The black markers show peak resistance R^p. (b) The peak resistance and the work needed to pass a ridge as function of the flare angle ψ, normalised by the results obtained for MT Uikku. (c) Snapshots from simulation for MT Uikku and the simple hulls 1 – 4 (dark grey) penetrating a narrow ridge (light grey) at the time instant of R^p.

We also analysed the relations of ridge resistance records and the ridge deformation patterns by using snapshots from simulations. Figure 3a shows that R^p of MT Uikku occurs earlier than

that of the simple hull forms. Figure 3c compares the snapshots from these stages and illustrates that the time instant of R^p is related to the bow length. For MT Uikku, R increases continuously until the bow fully interacts with the ridge. For the simple hull forms, R^p is achieved at a later stage, since their L_{bow} is longer than that of MT Uikku.

The effect of waterline angle α on ridge resistance

Figure 4a shows the R-δ records for the simple hull forms 4 – 6 with vertical bows, but different waterline angles α (Table 2). The data obtained with MT Uikku is shown for reference. The waterline angle α has a strong effect on both the features of the R-δ records and the magnitude of the peak ridge resistance R^p. Figure 4b illustrates that $\hat{R}^p$ – the peak resistance normalised by R^p of MT Uikku – has a linear relationship with α for these simple hull forms with vertical bows. A similar linear relationship with α is found for the normalised work $\widehat{W}$ done by these hulls when passing a ridge (δ = 0 … 80 m). When α increases from 15° to 45°, $\hat{R}^p$ more than doubles, but again, the change in $\widehat{W}$ is smaller. One of the simple hull forms (Hull 4) has the same α of 25.2° as MT Uikku at B/4, but R^p is about 50% higher than that of MT Uikku. This is because for Hull 4 both ψ = 90° and φ = 90°. Hull 4 uses similar work W as Hull 5 to pass through a ridge, but has a higher R^p.

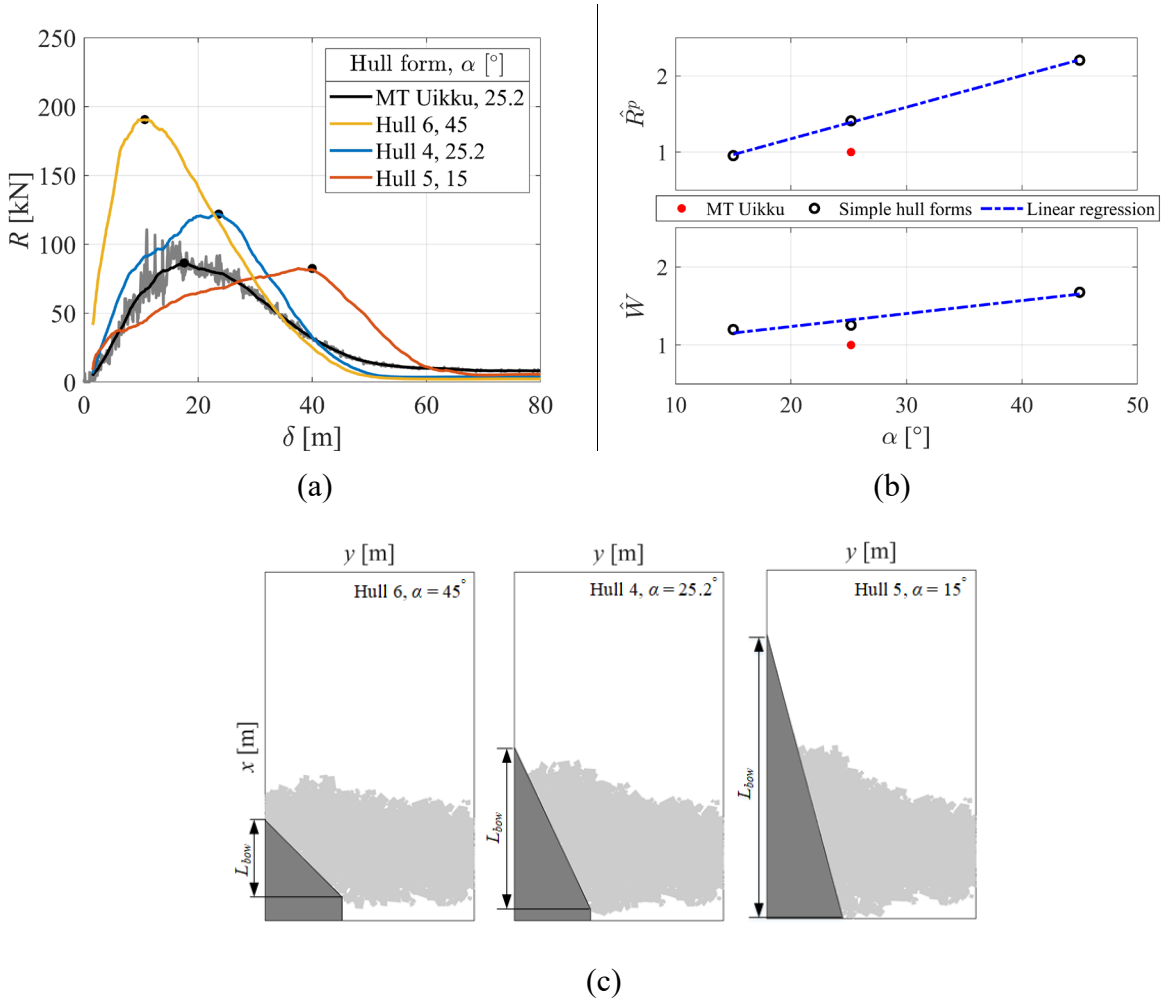

Figure 4. (a) Ridge resistance – ship displacement (R-δ) records for simple hull forms with vertical bows but varying waterline angle α (Hulls 4 – 6 in Table 2). The data for MT Uikku is given for reference. The unfiltered data for MT Uikku is coloured in grey. (b) The normalised peak ridge resistance $\hat{R}^p$ and work $\widehat{W}$ as a function of α. (c) Snapshot for each simple hull (dark grey) penetrating a narrow ridge (light grey) at the time instant of R^p, corresponding to the black marks in Figure 4a.

Figure 4c shows snapshots from the simulations. For each simple hull form, a snapshot of a view on *xy*-plane at the time instant of R^p is shown; R^p are marked with black dots in Figure 4a. The snapshots illustrate that R^p occurs when $\delta = L_{bow}$, that is, when the whole bow has indented into the ridge. This same observation was made also above. Hence, the stage when R^p is reached can be estimated from the bow length, at least for ships with a wedge shaped bow studied in this paper.

Based on the results above, we can conclude that a wedge shaped bow with a larger α can fail a narrow ridge more quickly but result in higher R, than a bow with a smaller α. This can be applied to explain how α affects the feature of R-δ for MT Uikku. Figure 3a shows that the rate of increase in R is first higher and then lower when R is approaching R^p. This is related to the change of α along the bow. A large α at the front bow disintegrates the ridge in a short time period and in return the rate of increase in R is high. Then, as α is gradually decreasing before the bow intermediate, the rate of increase in R decreases.

CONCLUSIONS

3D DEM simulations on a ship passage through a narrow ridge were performed with MT Uikku and ship hulls with a simple wedge shaped bows. The simulated ridge resistance records and snapshots from simulations show that the simple hulls yield similar ridge penetration processes as MT Uikku. For the simple hull forms, both the peak ridge resistance R^p and the work needed for passing a ridge are approximately linearly increasing with an increase in any of the bow angles. The work needed for a ship passing through a ridge appears less sensitive to changes in the hull form than the peak resistance.

ACKNOWLEDGEMENTS

We are grateful for the support from the Academy of Finland through the project Kara-Arctic Monitoring and Operation Planning Platform (KAMON).

REFERENCES

Gong, H., Polojärvi, A., & Tuhkuri, J., 2017. Preliminary 3D DEM simulations on ridge keel resistance on ships. In: The 24th International Conference on Port and Ocean Engineering under Arctic Conditions, *Proceedings of the 24th POAC conference*, pp. POAC17-091.

Gong, H., Polojärvi, A., & Tuhkuri, J., 2018. 3D DEM study on the effect of ridge keel width on rubble resistance on ships. In: ASME 2018 37th International Conference on Ocean, Offshore and Arctic Engineering, *Proceedings of the 37th OMAE Conference*, pp. V008T07A021-V008T07A021.

International Association of Classification Societies (IACS), 2016. *Requirements concerning Polar class*, London: IACS.

Keinonen, A., 1979. *An analytical method for calculating the pure ridge resistance encountered by ships in first year ice ridges*. Ph.D. Espoo: Teknillinen Korkeakoulu.

Kujala, P. & Riska, K., 2010. *Talvimerenkulku*, Espoo: Teknillinen korkeakoulu.

Kulyakhtin, S. & Høyland, K., 2014. Distribution of ice block sizes in sails of pressure ice ridges. In: The 22nd IAHR International Symposium on Ice, *Proceedings of the 22nd IAHR International Symposium on Ice*, pp. 235-240.

Li, H., Feng, Y., Yang, Z., Sheng, W., & Qian, Y., 2018. Study on influence of bow configuration on dynamic response of ship collision with ice. In: ASME 2018 37th

International Conference on Ocean, Offshore and Arctic Engineering, *Proceedings of the 37th OMAE Conference*, pp. V008T07A018-V008T07A018.

Lindqvist, G, 1989. A straightforward method for calculation of ice resistance of ships. In: The 10th International Conference on Port and Ocean Engineering under Arctic Conditions, *Proceedings of the 10th POAC conference*, pp. 722-735.

Malmberg, S., 1983. *Om fartygs fastkilning i is*. Master. Espoo: Teknillinen Korkeakoulu.

Myland, D. & Ehlers, S., 2016. Influence of bow design on ice breaking resistance. *Ocean Engineering*, 119, pp. 217-232.

Palmer, A. & Croasdale, K., 2013. *Arctic offshore engineering.* World Scientific: Singapore.

Polojärvi, A. & Tuhkuri, J., 2009. 3D discrete numerical modelling of ridge keel punch through tests. *Cold Regions Science and Technology*, 56(1), pp. 18–29.

Polojärvi, A., Tuhkuri, J., & Korkalo, O., 2012. Comparison and analysis of experimental and virtual laboratory scale punch through tests. *Cold Regions Science and Technology*, 81, pp. 11-25.

Riska, K., 2014. *Factors influencing the power requirement in the Finnish-Swedish ice class rules*. Helsinki: Finnish Maritime Administration.

Transport Safety Agency (TRAFI), 2010. *Finnish-Swedish Ice Class Rules 2010*, Helsinki: TRAFI.

Yamaguchi, H., Suzuki, Y., Uemura, O., Kato, H., & Izumiyama, K., 1997. Influence of bow shape on icebreaking resistance in low speed range. In: The 16th International Conference on Offshore Mechanics and Arctic Engineering / 14th International Conference on Port and Ocean Engineering under Arctic Conditions (Joint OMAE/POAC Conference), *Proceedings of the 16th OMAE Conference / 14th POAC Conference*, pp. 51-62.